The 2016 World Congress on
Advances in Civil, Environmental, and Materials Research (ACEM16)
Jeju Island, Korea, August 28-September 1, 2016

Numerical Study of the Flow in the Near-Wake of a Flapping Airfoil

*Jiawei Wan[1)] and Haili Liao[2)]

[1), 2)] *Research Center for Wind Engineering, Southwest Jiaotong University, Chengdu 610031, China*
[1)] *jiawei.wan@outlook.com*

ABSTRACT

The flow field in the near wake of a NACA-0012 airfoil pitching harmonically at small amplitude is numerically simulated in the present study. The characteristics of vortical patterns, i.e. the formulation and downstream evolution of vortex, and its relationship with the reduced frequency are investigated. The pressure variation along the chord surface are also computed to study the connection between wake structure and drag-to-thrust transition. The numerical results highlight the wake structure consists of an array of alternating vortex and its dependence on oscillating frequency. Note that, the transverse location of vortex array changes from an orientation leading to velocity deficit (Von Kármán street with wake profile) to one with velocity excess (reverse Von Kármán street with jet profile) with increasing reduced frequency. However, the switch from Von Kármán vortex street to reverse Von Kármán vortex street is found to take place ahead of the drag-to-thrust transition. Interesting features regarding to the initial formulation and evolution of vortex are also demonstrated and attempts are made to account for the relating phenomenon.

1. INTRODUCTION

The aerodynamic characteristics of a flapping airfoil and its wake structure has received massive attention over the past few decades as a consequence of the interest in solving aircraft flutter, buffeting and dynamic stall problems. Extensive researches with biological applications focusing on flapping wing propulsion have also been carried out to study this subject. Moreover, there has been a surge interest in bio-inspired flapping wing kinematics because of the potential applications in the design of micro-air vehicle.

In comparison with the many theoretical, experimental and numerical studies that have been mostly concentrated on measuring the forces on oscillating wings, the characteristics of wake structure and its connection with flapping airfoil aerodynamics seems to have received lesser attention. The wake structure of flapping airfoil is highly

[1)] Graduate Student
[2)] Professor

vortical and closely linked with a variety of fundamental parameters such as motion type (e.g. pitch and heave), oscillating amplitude and frequency. A comprehensive understanding of the generation of vorticity, its shedding and subsequent evolution is of great importance for a theoretical understanding of the drag-thrust transition and its relationship with the corresponding vortical pattern. Among the available experimental investigation which mostly utilized flow visualization, the vorticity field in the near wake of flapping airfoil could only be qualitatively inferred rather than quantitatively measured. Although, the whole-field velocimetry methods (i.e. PIV, MTV) are now utilized to quantify the characteristics of vortical field (Bohl et al. 2009), there are spatial and temporal resolution challenges involved in vorticity measurement that remain to be solved.

As the geometry of airfoil with small dimension however precludes the direct measurements of surface pressure variation, the estimation of mean aerodynamics has been conducted mostly in terms of wake flow statistics. By applying the integral momentum theorem to a control volume surrounding the oscillating airfoil, the mean drag/thrust forces can be derived based on mean streamwise velocity profiles only with the velocity fluctuation and pressure terms neglected. However, the accuracy of aforementioned approaches is questioned as a consequence of the increase in velocity fluctuation and the decrease in wake pressure with ascending oscillating frequency. Compared to conventional experimental approaches, the numerical simulation could provide a detailed analysis of the vortical field in the wake of flapping airfoil with a sufficient spatial resolution near the trailing edge, and compute the aerodynamic forces acting on airfoil directly on the basis of pressure variations.

The study presented here focuses on quantifying the properties of the vortical field in the near wake of NACA-0012 airfoil subjected to harmonic pitching motion at a constant amplitude with various reduced velocity at a chord-width based Reynolds number Re_C = 12600. The emphasis is primarily on the transitions from the Von Kármán vortex street to the reverse Von Kármán vortex street, which is closely related to the drag-to-thrust transition. A detailed spatial analysis of the formulation of vortex array and its peak magnitude evolution over the first chord length is conducted to investigate the connection between those properties and generation of thrust. The aerodynamic forces and surface pressure distributions on pitching airfoil are also computed as a supplement. A high resolution mesh grid system is utilized within the trailing edge and near wake region to ensure the high fidelity of the computed wake vorticity field. Also note that the flow is laminar for the Reynolds number considered here, no turbulence model is applied in the numerical simulation.

The paper is organized as follows. An overview of the computational setup, grid system, numerical schemes and post processing are given in Section 2. Discussions of results are presented in Section 3.1 for the detailed behavior of the vortical field, followed by the aerodynamic forces and surface pressure variation is presented in Section 3.2.

2. COMPUTATIONAL SETUP

The geometry of airfoil, having a chord width C, utilizes the NACA-0012 profile. Simulations of the flow field are carried out on an elongated C-type structured mesh. The computational domain having the origin at the tip of trailing edge is illustrated in Fig. 1 along with the boundary conditions implemented in this study. The first cell distance from the airfoil surface is set equal to 1×10^{-3}C with a homogeneous chord-wise resolution of 4×10^{-3}C. The gird is then uniformly stretched in the normal direction of airfoil surface with a stretching factor of 1.02 inside the C-type grid. A total number of 601 grid points in the circumference and 181 grid points in the radial direction are distributed for the C-type grid around the airfoil. A close-up view of mesh grid in the vicinity of airfoil is shown in Fig. 2.

The Dirichlet condition on the velocity field is imposed at the inlet boundary with the velocity of parallel free stream set to U_0, yielding a chord-width based Reynolds number $Re_C = U_0C/v = 12600$ to cope with the conditions reported in D. G. Bohl et al. (2009). The Neumann boundary condition with $\partial U/\partial x = 0$ is applied at the outlet boundary. Periodic condition are imposed on the side surfaces. No slip condition is applied at the foil surface. Pressure on the perimeter of the computational domain and its normal derivative on the wall boundary are set to zero.

The filtered incompressible Navier-Stokes equations are integrated on a collocated grid using the finite-volume method. To avoid the generation of a checkerboard problem, the modified Rhie-Chow velocity interpolation procedure is utilized which allows the formulation of the SIMPLE algorithm on a collocated grid. The Bounded Central Differencing Scheme is applied for diffusion and convection schemes. The least square method is employed for the computation of gradients at cell centroids which offers more flexibility with regard to the order of accuracy it achieved. For the discretization of the temporal term, a Second-order Upwind Euler Scheme (SOUE) is utilized. The time is non-dimensionalised by U_0 and C, with the non-dimensional time-step set equal to $\Delta t = 3\times10^{-4}$, providing an accurate advancement in time and a CFL number below unit.

To investigate the transition from the Von Kármán wake to the reverse Von Kármán wake with increasing oscillation frequency, the airfoil is subjected to a sinusoidal pitching-motion about its 1/4–C axis with an amplitude α_0 of 2° (i.e. peak to peak amplitude of 4°) about a zero mean angle of attack (AOA) and a reduced frequency $k = 2\pi fC/2U$ in the range of 5.2~11.5. The flow field under investigation is periodic and could, therefore, be phase averaged quite effectively. In this work, each case is divided into 40 phases and then averaged. The data-processing strategy allows the data from multiple field of views to combined into one single data set to create the evolution of flow field map versus oscillating phase for each reduced frequency. Phase-averaged quantities are indicated by bracketed <> variables.

The statistics are accumulated over eight oscillating cycle after having excluded the initial transient. Computations are carried out on 8 Intel Xeon E5 2696V3 2.8GHz

CPUs and require about 2GB of RAM memory and 7 days of CPU time for the whole simulation.

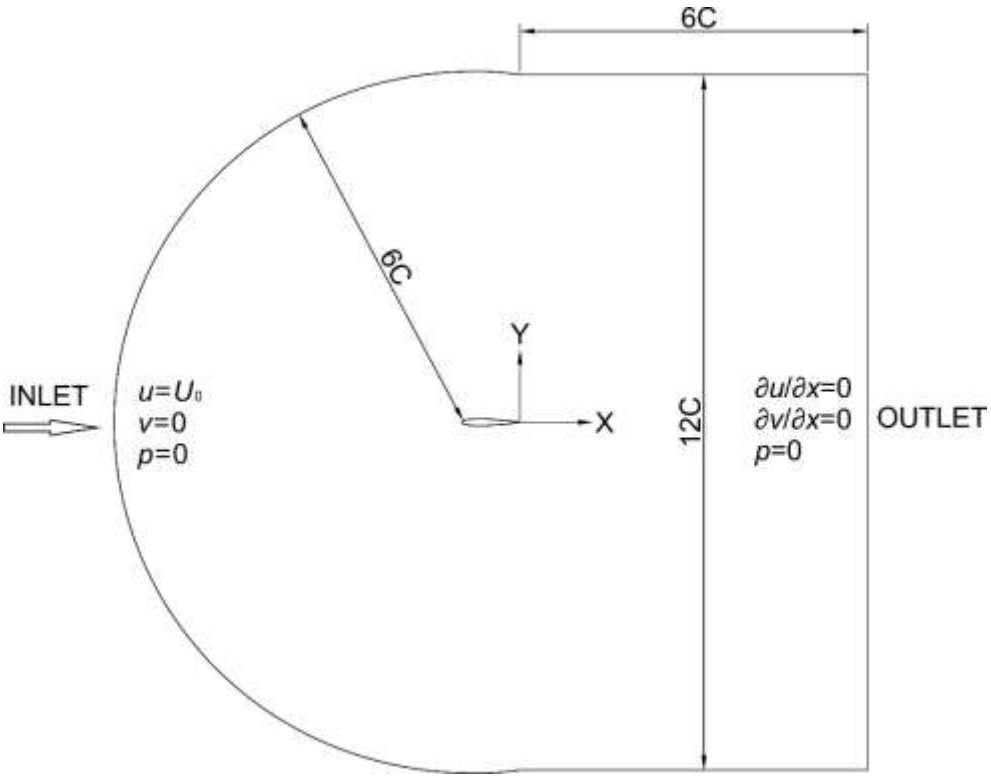

Fig. 1 Computational domain and boundary conditions

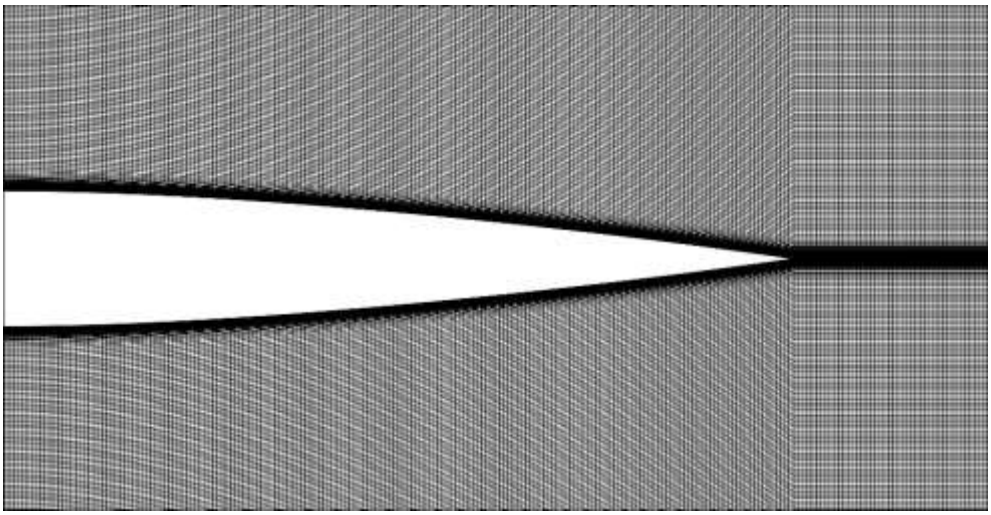

Fig. 2 Mesh grid system in the vicinity of airfoil

3. RESULTS AND DISCUSSIONS

3.1 Vorticity field

The results discussed here are demonstrated over a downstream distance of $0<x/C<1.0$. The origin of coordinates is placed at the airfoil trailing edge with the airfoil at the zero angle of attack. The out of plane vorticity ω_z is calculated from the computed (u, v) velocity field using a fourth order accurate central finite differencing scheme (Cohn and Koochesfahani, 2001) to quantify the wake structure of pitching airfoil. The phase-averaged non-dimensional vorticity fields $<\omega_z>C/U_0$ for stationary and oscillating airfoil with three reduced frequencies of k = 5.2, 5.7 and 11.5 are shown in Fig. 3. These specific cases are selected for discussion because they highlight the essential features of the wake transition and to cope with Bohl's experiment (2009).

The vorticity plots suggest that the boundary layers along the two sides of airfoil and the trailing edge experiencing the pitching oscillating are the two sources of vorticity generation, in which the vorticity production at the trailing edge depends on the frequency and amplitude of oscillations. An array of isolated vortices of alternating sign can be identified in the tested reduced frequencies, whereas the significant distinction among them is the transverse arrangement of vortical pattern. To quantify the transverse location of isolated vortices and following Bohl's notation (2009), the core of a vortex is defined by the coordinates (x_c, y_c) of its peak vorticity. Thus, the vortex array can be characterized in terms of its transverse spacing b defined as $b \equiv y_{c,p} - y_{c,n}$ where $y_{c,p}$ and $y_{c,n}$ are the transverse location of positive (clockwise circulation) and negative (clockwise circulation) vortices.

For k = 5.2, the vortex with a negative circulation is located on top ($y_{c,n} > 0$) while the one with positive circulation on the bottom ($y_{c,p} < 0$). This vortical pattern results in $b < 0$ and exhibits a typical Von Kármán vortex street observed in the wake profile with a velocity deficit. For k = 11.5, the vortex with a positive circulation is located on top ($y_{c,p} > 0$) while the one with negative circulation on the bottom ($y_{c,n} < 0$). This vortical pattern results in $b > 0$ and exhibits a typical reverse Von Kármán vortex street observed in the jet profile with a velocity excess. However for k = 5.7, the vortices of alternating sign are nearly aligned along the centreline $y = 0$ (i.e. $y_{c,p} \approx y_{c,n}$, $b \approx 0$) resulting a uniform streamwise velocity profile. The rearrangement of the transverse positions of the vortices in the vortex street with increasing frequency is consistent with the previous findings arrived by molecular tagging velocimetry (D. G. Bohl et al., 2009) and flow visualization (Koochesfahani, 1989).

Another remarkable characteristics of vorticity fields is the existence of a thin vorticity layer, i.e. braid, that connects the isolated shedding vortices (see the right column in Fig. 3 with contour levels adjusted to highlight the braid regions). The thickness of the braids and its vorticity level shown in the contours decrease with downstream distance at different rates depending on oscillating frequency. For low reduced frequency case, k = 5.2, the well-resolved braid regions can be identified within and over the first chord length. On the contrary, no connecting vorticity could be found beyond the first pair of vortices in high reduced frequency case, i.e. k = 11.5. The

vorticity plots also suggest that the downstream formation length of vortices decreases with increasing reduced frequency.

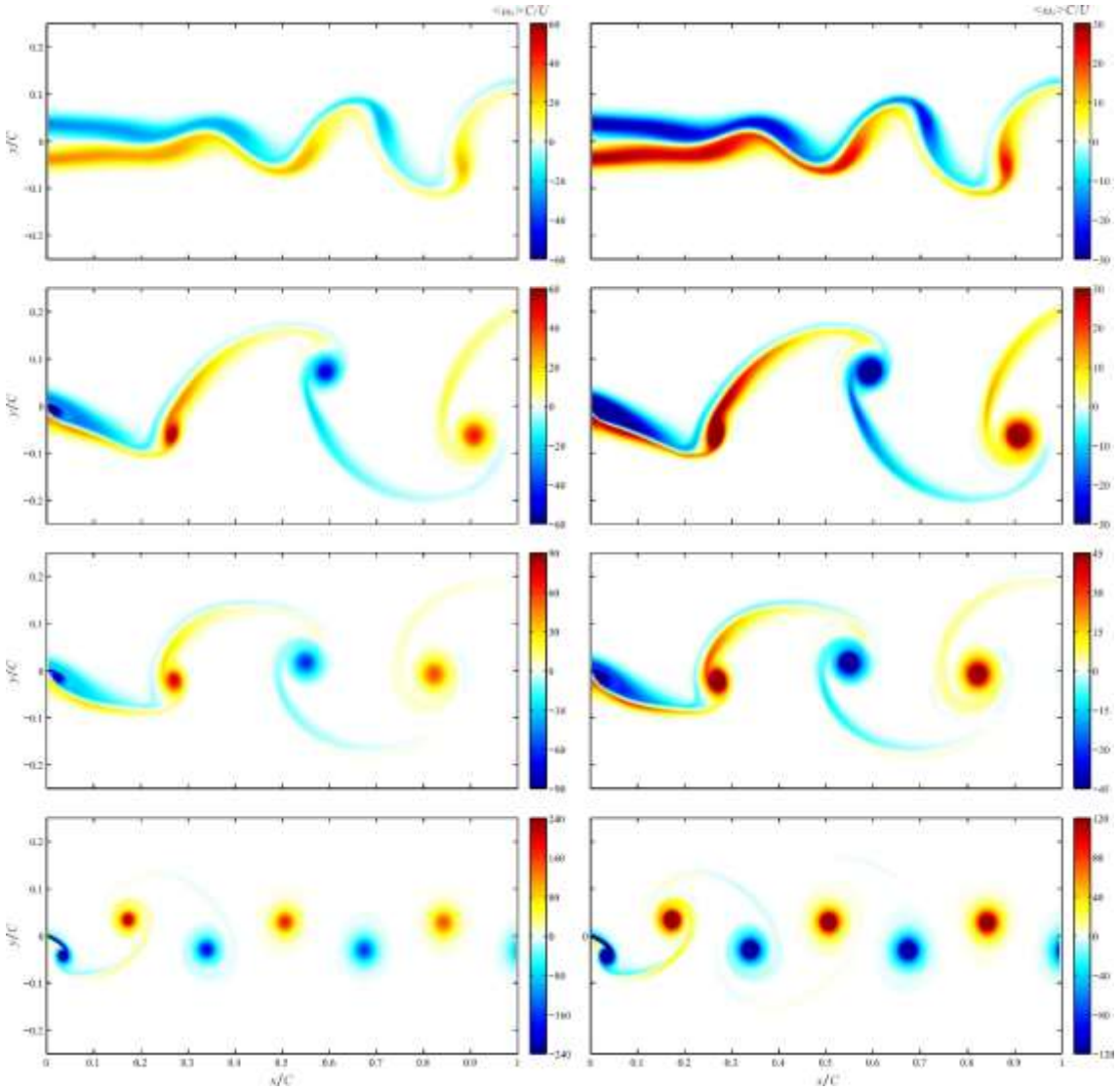

Fig. 3 Phase-averaged vorticity contours in the near wake of static and pitching airfoil.

The non-dimensional mean and fluctuating vorticity, $\omega_{avg}C/U_0$ and $\omega_{r.m.s.}C/U_0$ for oscillating airfoil with three reduced frequencies of k = 5.2, 5.7 and 11.5 are shown in Fig. 4. The mean and r.m.s. vorticity fields of the stationary airfoil at zero AOA are also demonstrated as a supplement. In the case of stationary airfoil, the boundary layer vorticity initiating from the sides of airfoil left the trailing edge quite steadily into the near wake while reducing in peak level with downstream evolution. The mean vorticity fields of low reduced frequency case (k = 5.2) was characterized by the transverse spreading and downstream decaying of braid regions initiated from the trailing edge. The mean vorticity within these regions is of opposite sign to the corresponding boundary later vorticity on the same side. Two well-defined mean vorticity peaks of opposite sign can be identified in second half chord downstream distance where the isolated vortices

have formed in this region. The spacing between the peaks initially increases, followed by a decrease to an asymptotic value by x/C = 1.

The aforementioned behaviors about the characteristics of the mean vorticity field in the near wake region also holds for the case of k = 5.7. The unique feature of this case is the fact that the mean vorticity is nearly zero for x/C > 0.75 indicating the perfect alignment of alternating vortices. In the high reduced frequency case (k = 11.5), two well-defined peaks of opposite sign right at the trailing edge is developed in the mean vorticity filed, indicating the rapid shedding of the isolated vortices at trailing edge. A wavy pattern can be identified for the spacing between the mean vorticity peaks in the near wake before it reaches to a fixed spacing in the far wake. The r.m.s. vorticity field also shows the same initial wavy pattern existed in the mean vorticity.

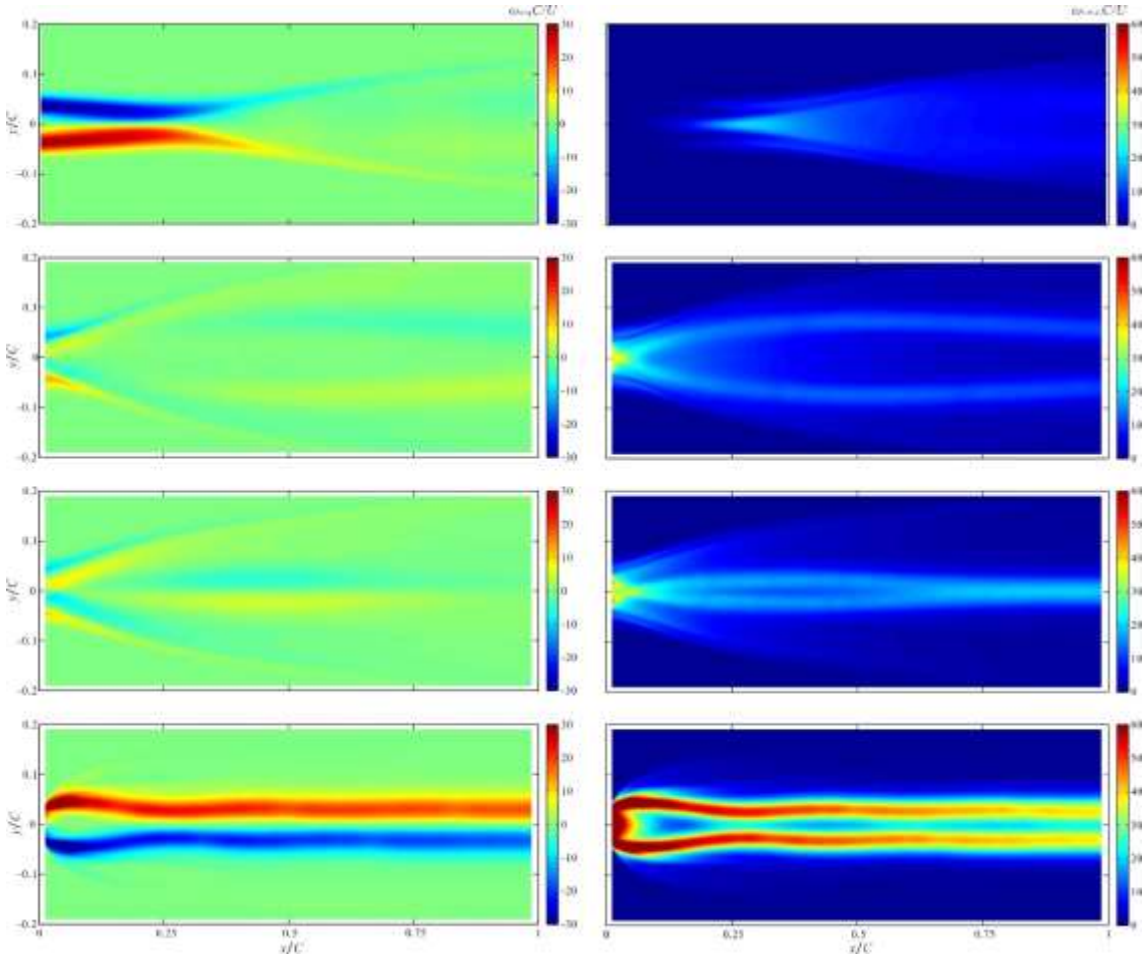

Fig. 4 Mean and r.m.s. vorticity fields, ω_{avg} and $\omega_{r.m.s.}$ in the near wake of static and pitching airfoil

The downstream evolution of vortex spacing as derived from tracking the trajectories of individual vortices is presented to provide a quantitative assessment of the vortical patterns. The computed variation of the transverse coordinates of positive and negative vortices, $y_{c,p}$ and $y_{c,n}$, along with the vortex array transverse spacing is

illustrated in Fig. 5. The variation of of peak vorticity $<\omega_z>_{peak}$ as a function of vortex core downstream location x_c is also demonstrated (see Fig. 6). In the low reduced frequency case (k = 5.2), the positive vortices are initiated at y > 0 whereas the negative vortices are initiated at y < 0. Then, the vortex array start to move towards each other and reaches to an orientation switch at $x/C \approx$ 0.03C. After that, the vortex array moves apart over the first half chord downstream to a maximum spacing of about b = 0.15C before moving back towards each other again and approaching a constant transverse spacing at about x/C = 1 with negative vortex on top. In the high reduced frequency case, the vortex array transverse spacing possesses a oscillatory behavior with a maximum amplitude of only about 0.01C. The oscillation damped out quickly and the vortical pattern attains a transverse spacing with positive vortices on top.

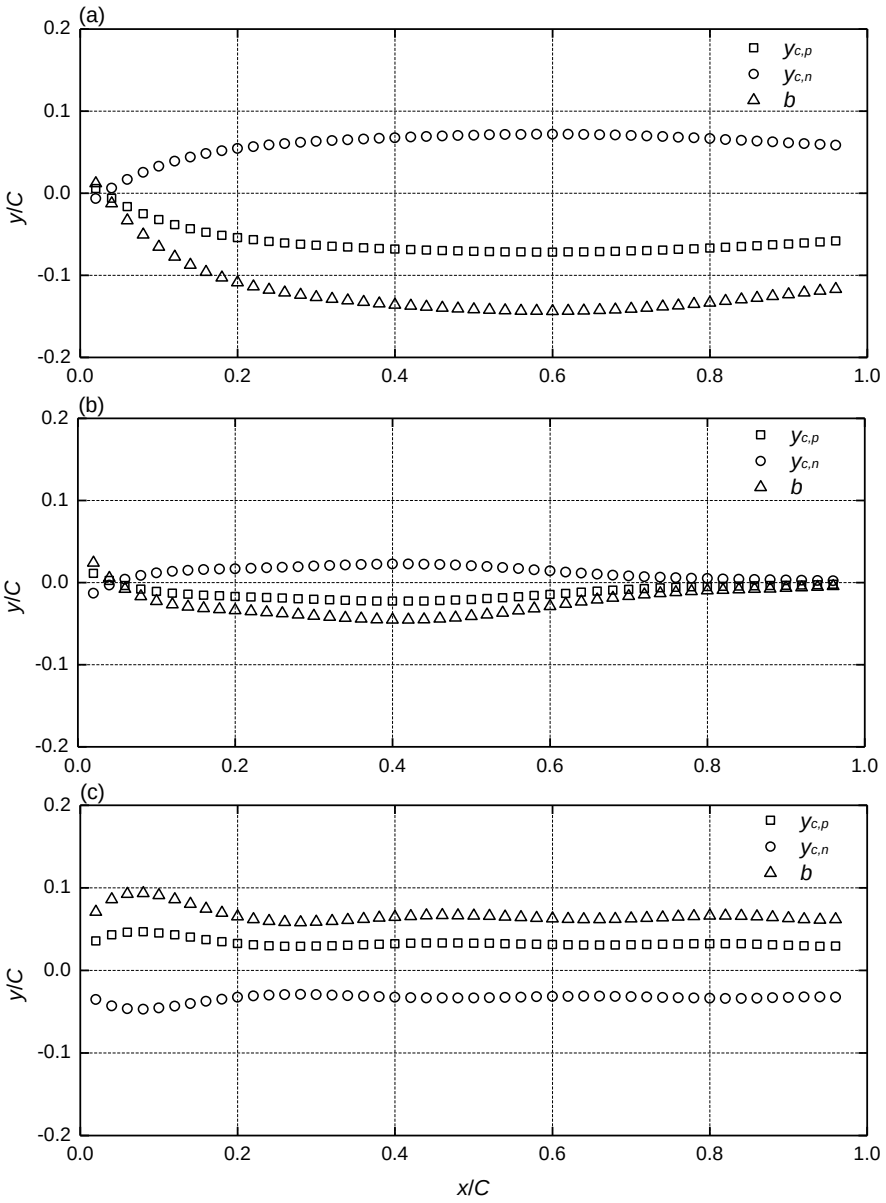

Fig. 5 Downstream evolution of vortex coordinates: (a) k=5.2, (b) k=5.7 and (c) k=11.5

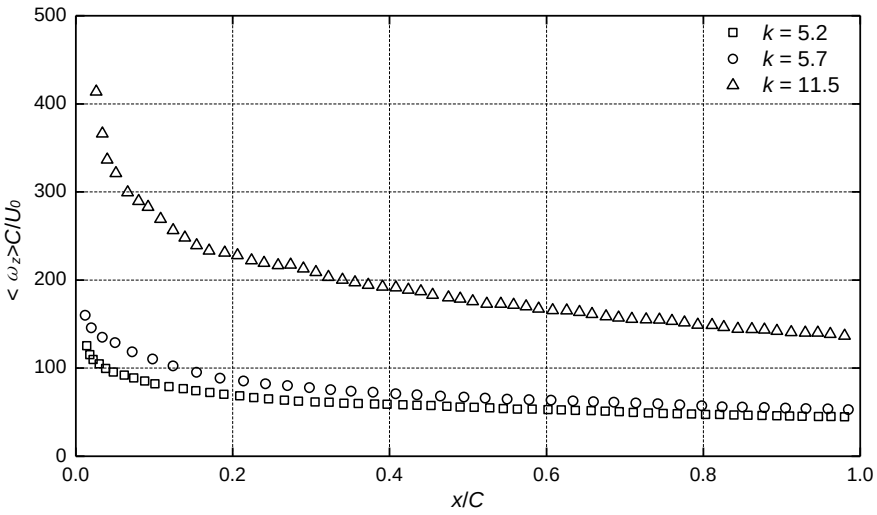

Fig. 6 Peak vorticity $<\omega_z>_{peak}$ as a function of as a function of vortex core downstream location for k = 5.2, 5.7 and 11.5

3.2 Aerodynamics and pressure variations

The streamwise aerodynamic force acting on the pitching airfoil (i.e. drag or thrust) are computed by integrating the surface pressure along the chord surface, and is shown in Fig. 7. The areodynamic hysteresis are also demonstrated as a supplement (Fig. 8). A large increase in thrust peak is identified for reduced frequency k = 11.5 and the thrust peak is found to be reached when the airfoil is at its maximum pitching amplitude. The mean pressure coefficient along the airfoil is also shown (Fig. 9) to explore the connection between drag-to-thrust transition with surface pressure variation. For k = 5.2 or 5.7, the C_P plot resemble that of static foil within almost the entire chord length except for trailing edge where the suction pressure increases. However, for k = 11.5, a significant increase in negative pressure peak is demonstrated which highlights the massive generation of vorticity at this region.

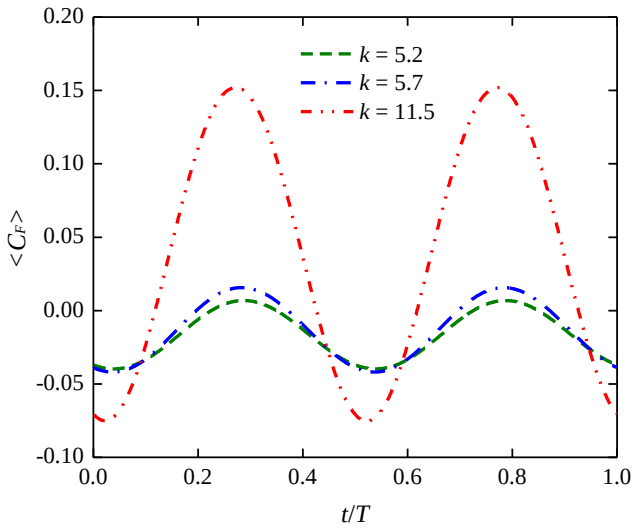

Fig. 7 Time histories of the streamwise force coefficient for k = 5.2, 5.7 and 11.5

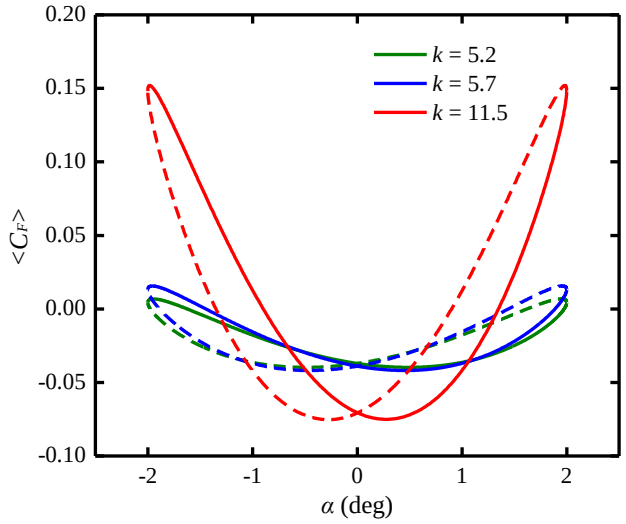

Fig. 8 Aerodynamic hysteresis of the streamwise force coefficient for k = 5.2, 5.7 and 11.5 (solid lines denote upstroke, dashed lines denote downstroke)

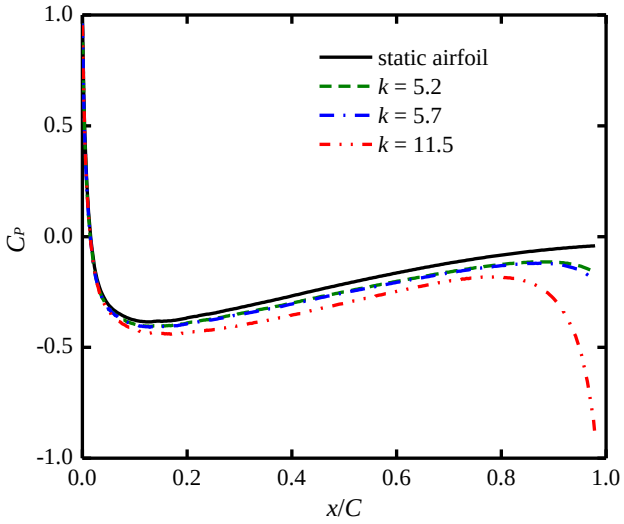

Fig. 9 Mean surface pressure coefficient along the airfoil for k = 5.2, 5.7 and 11.5

4. CONCLUSIONS

The flow field in the near wake of a NACA-0012 airfoil pitching harmonically at small amplitude is numerically simulated in the present study. The characteristics of vortical patterns, i.e. the formulation and downstream evolution of vortex, and its relationship with the reduced frequency are investigated. The pressure variation along the chord surface are also computed to study the connection between wake structure and drag-to-thrust transition. The numerical results highlight the wake structure consists of an array of alternating vortex and its dependence on oscillating frequency. Note that, the transverse location of vortex array changes from an orientation leading to velocity deficit (Von Kármán street with wake profile) to one with velocity excess (reverse Von

Kármán street with jet profile) with increasing reduced frequency. However, the switch from Von Kármán vortex street to reverse Von Kármán vortex street is found to take place ahead of the drag-to-thrust transition.

REFERENCES

Schnipper, T., Andersen, A., Bohr, T. (2009), "Vortex wakes of a flapping foil", *J. Fluid Mech.,* **633**, 411-423.

Jeong, J., Hussain, F. (1995), "On the identification of a vortex", *J. Fluid Mech.,* **285**, 69-94.

Cohn, R. K. & Koochesfahani, M. M. (2000), "The accuracy of remapping irregularly spaced velocity data onto a regular grid and the computation of vorticity", Experiments Fluids **29**, S61.

Koochesfahani, M. M. (1989), "Vortical patterns in the wake of an oscillating airfoil", AIAA J. **27**,1200.

Bohl, D. G. & Koochesfahani, M. M. (2009), "MTV measurements of the vortical field in the wake of an airfoil oscillating at high reduced frequency", J. Fluid Mech. **620**, 63-88.